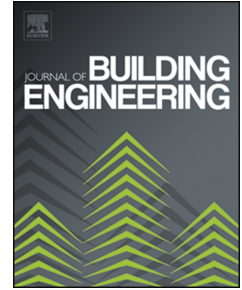


Journal Pre-proof

LONG-TERM field study of a Waterborne paint with a nano-additive for biodeterioration control

Erasmus Gámez-Espinosa, Cecilia Deyá, Facundo Ruiz, Natalia Bellotti



PII: S2352-7102(22)00161-9

DOI: <https://doi.org/10.1016/j.jobe.2022.104148>

Reference: JOBE 104148

To appear in: *Journal of Building Engineering*

Received Date: 19 November 2021

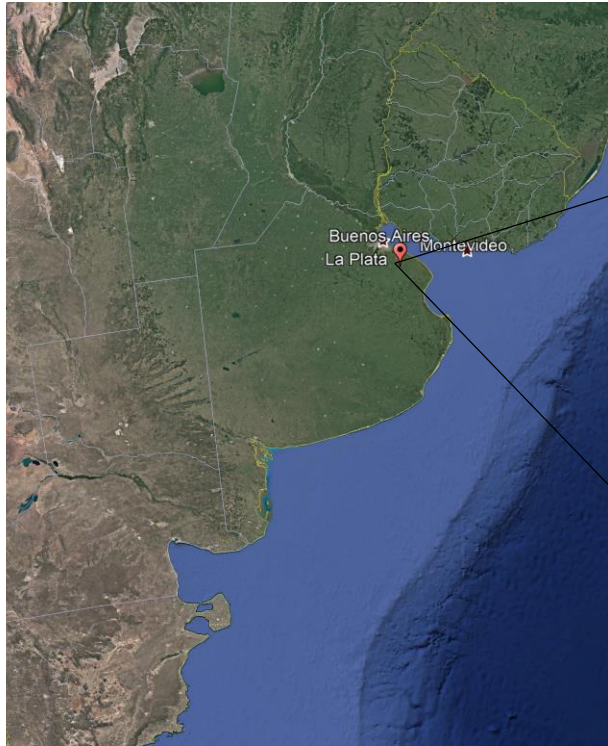
Revised Date: 28 January 2022

Accepted Date: 29 January 2022

Please cite this article as: E. Gámez-Espinosa, C. Deyá, F. Ruiz, N. Bellotti, LONG-TERM field study of a Waterborne paint with a nano-additive for biodeterioration control, *Journal of Building Engineering* (2022), doi: <https://doi.org/10.1016/j.jobe.2022.104148>.

This is a PDF file of an article that has undergone enhancements after acceptance, such as the addition of a cover page and metadata, and formatting for readability, but it is not yet the definitive version of record. This version will undergo additional copyediting, typesetting and review before it is published in its final form, but we are providing this version to give early visibility of the article. Please note that, during the production process, errors may be discovered which could affect the content, and all legal disclaimers that apply to the journal pertain.

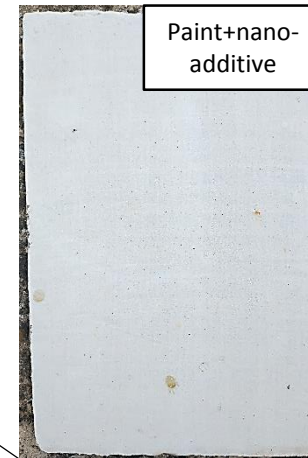
© 2022 Published by Elsevier Ltd.



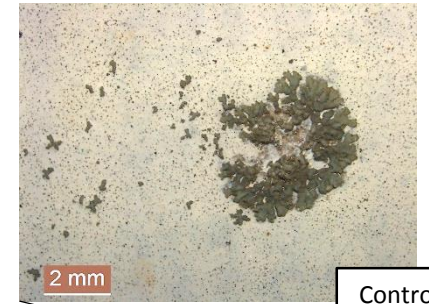
© 2020 Google
US Dept of State Geographer
Data SIO, NOAA, U.S. Navy, NGA, GEBCO



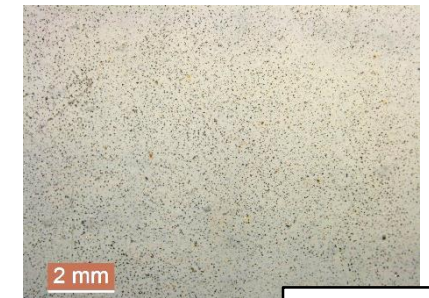
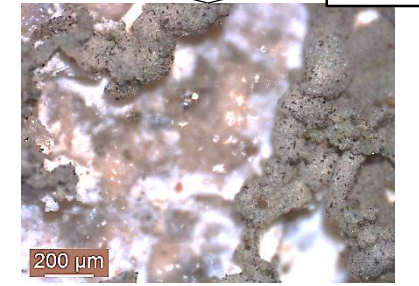
After 4 years
North orientation



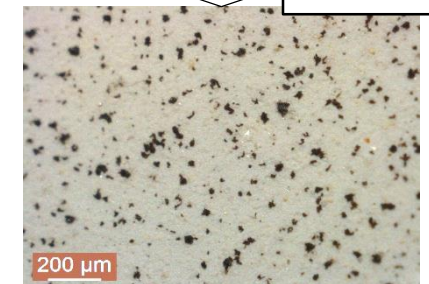
Stereomicroscope images



Control paint



Paint+nano-additive



LONG-TERM FIELD STUDY OF A WATERBORNE PAINT WITH A NANO-ADDITIVE FOR BIODETERIORATION CONTROL

Erasmus Gámez-Espinosa¹, Cecilia Deyá^{1,2}, Facundo Ruiz³, Natalia Bellotti^{1,4*}

¹ Centro de Investigación y Desarrollo en Tecnología de Pinturas (CONICET-CICPBA-UNLP), Buenos Aires, Argentina

² Facultad de Ingeniería-Universidad Nacional de La Plata, Buenos Aires, Argentina

³ Universidad Autónoma de San Luis Potosí, San Luis Potosí, México

⁴ Facultad de Ciencias Naturales y Museo-Universidad Nacional de La Plata, Buenos Aires, Argentina

* e-mail: n.bellotti@cidepint.ing.unlp.edu.ar

ABSTRACT

Biodeterioration in building façades represents an important economic loss related to maintaining a functional protective coating system. Research papers with long-time studies on paint performance exposed to field conditions are scarce. Fungi, cyanobacteria, and algae are frequently present in biofilms formed in outdoor locations. Among these, defacement caused by fungi is known for the broad damage spectrum produced. Therefore, it is important to extend the service life of the protective coatings systems. To reach this goal, studies that consider the action of both biotic and abiotic factors acting simultaneously for prolonged periods are necessary. The present research work presents the assessment carried out on acrylic outdoor paint with a nano-additive exposed to long-term field conditions. Paint with 1% by weight of ZnO particles with nano-sized crystallites (nano-additive) was exposed to natural weathering. Samples with north and south orientation were evaluated by long-term field studies during a period of four years. The incorporation of the nano-additive proved to extend service life. In the paints facing north, the ZnO particles were more efficient for the biodeterioration control.

Key words: waterborne paint, nano-additive, biodeterioration, natural weathering, service life

1. INTRODUCTION

Paints are dispersed systems that, when applied to a material, form a film with protective and aesthetic purposes [1]. In general, they contain the same basic constituents: binder, pigments, extenders or fillers, additives, and solvent. They can be classified based on the binder which could

be inorganic-like on silicate paints or organic with polymers such as alkyd, acrylic or poly (vinyl acetate) [2]. Waterborne acrylic paints have become those most used in architectural protective systems due to an efficient cost / benefit ratio, low VOC, odor and toxicity [3]. These coatings undergo the greatest challenge when exposed outdoors given the diversity of abiotic and biotic factors such as sun radiation, rainwater, winds, pollutants, and micro- and macro-organisms, among others. Although paint formulations are thought to face environmental conditions, they often fail showing their limitations in service life [4]. The failure rate in the service life of building materials has negative consequences such as economic and energy losses. Rauf and Crawford showed that the longer a building lasts, the lower its annual life cycle embodies energy demand; in this sense, the coating protective systems can play an important role [5]. A critical analysis of several studies about painted surfaces from exterior façades, recently published, has shown a high variation between the estimated service life values, ranged from 3 to 60 years [6]. The wide range of these values can be attributed to differences in the methodology and models used in the studies, regions with diverse climatic conditions and paint formulations. In general, many of the studies consider building painted surfaces. There are few references to studies carried out with paint films samples tested in natural environment prior to their commercialization. Therefore, more studies integrating field tests are necessary.

Considering the components of the paint formulations, they are affected at different levels. Among these, binder degradation is extremely important since film forming material maintains the integrity of the coating. Styrene-acrylic binders absorb in the ultraviolet range (UV) leading to chain breakage and oxidation with formation of hydroperoxides, hydroxyl and carbonyl groups [7]. Binder degradation together with changes in material temperature leads to photo-chalking [8]. Another important issue is attributed to the leaching of antimicrobial additives (biocides) from the coatings by the action of rainfall, which has been studied in the last decades [9,10]. High cumulated active substances such as diuron, carbendazim and octylisothiazolinone (OIT) were found in the runoff from evaluated façades [11]. On the other hand, organic biocides that usually integrate commercial formulations, can be utilized as carbon source by some microorganisms [12]. Therefore, all these factors progressively reduce the biocide content of the film facilitating the colonization by microorganisms (fungi, bacteria and algae) that usually form biofilms on painted building materials. From the point of view of biodeterioration, fungi are the most damaging microorganisms (among those microorganisms) to paint films [4,13]. Once they manage to colonize the material, their growth is not limited to the surface line but rather they invade the material while releasing a large amount of highly degrading extracellular compounds. Fungal hyphae penetrate and widen fissures in rocks and

building materials and produce a broad range of enzymes, acids and pigments which cause erosion, degradation and discoloration [14,15]. The consolidation of the biofilm allows fungi to tolerate environmental stresses and exposure to biocides [16].

The failure of protective systems, apart from causing economic losses, produces a significant impact on the environment that must also be considered. In this sense, biocides combination (carbendazim, diuron and OIT) for outdoor formulations have recently been restricted due to their toxic and carcinogenic effect on environment and health [17]. In this sense, avoiding the loss of antimicrobial activity of paint films is an issue that has different approaches: use of inorganic bioactive additives, functional components that retain the active agent, structural design at nano or micrometric level of the surface, encapsulation of traditional biocides in siliceous matrices, to mention some of the strategies under study nowadays [17–20]. Many of these efforts are framed in the field of smart coatings which have become increasingly popular due to their functional properties that enable them to react to environmental stimuli, conferring, for example, magnetic, self-cleaning, anti-microbial and anticorrosive properties [21].

Among the active inorganic compounds thoroughly studied, ZnO nanoparticles (NPs) are highly promising due to their antimicrobial, photochemical and UV filtering activity. Based on their properties, they have been widely used in cosmetic and sunscreen industry and even as food additives [22]. The UV-shielding ZnO NPs property results promising in coating technology. These NPs could spread their activity to the protective system, increasing the resin resistance to photo-chalking and fungal growth [23,24]. This would be consistent with the efforts to extend the service life of outdoor paints. Therefore, it is necessary to develop studies that deepen the study of the formulations in natural conditions for long periods to improve the efficiency and materialization of functional designs. In addition, taking into account the concern for the environment, it is necessary to focus efforts on obtaining protective films with long service life, but that, at the same time, comply with the regulatory framework [2]. In addition to reducing the economic losses, the lengthening of the coating service life decreases the production of waste discharged into the environment.

The present research work proposes, for the first time, the evaluation of a water-based acrylic paint with ZnO particles exposed to outdoor long-term field conditions for four years. Paint samples were evaluated for biodeterioration, color, gloss, and contact angle. Bio-resistance was evaluated using conventional microbiological methods and microscopy techniques. Temperature measurements, Fourier transform infrared spectroscopy (FTIR), stereomicroscopy (SM), and scanning electron microscopy (SEM) observations were performed on the prepared paint films.

2. MATERIALS AND METHODS

2.1 Synthesis of the ZnO particles

The ZnO particles were obtained by precipitation in an aqueous alkaline medium. At first, 1.4 g of ZnCl₂ was added to 100 mL of deionized water in the reactor where drops of concentrated HCl were added until the solution clarified and homogenized with stirring for 10 min. Polyvinylpyrrolidone (PVP) was added as a stabilizer in a ratio of 0.057 g per g of ZnCl₂ and the stirring was maintained for 10 min. PVP acts both as a capping ligand and a size-controlling agent, its use facilitates the dilution of nanoparticles in various organic solvents without aggregation [25]. Then, 10 mL of precipitating agent (NaOH 2 M) were added while stirring for 30 minutes. Finally, 200 mL of NH₄OH were added. The final pH reaction was 8.5 and the synthesis temperature ~25°C. The product obtained was filtered, washed at least 3 times using ethanol and dried at room temperature.

2.2 Characterization

The ZnO particles were characterized by UV-Vis spectroscopy in Oceanoptics S2000 equipment in transmission mode to obtain the absorbance spectrum. The ZnO particles were analyzed using the originally obtained aqueous dispersion. Dynamic light scattering (DLS) technique was carried out to confirm particle size distribution. Size distribution measurements were made in triplicate with a Malvern Zeta sizer Nano ZS Instruments operating with a He-Ne laser at a wavelength of 633 nm and a detection angle of 90°; all samples were analyzed for 60 s at 25 °C. The same equipment was used to determine the Zeta potential (ZP). Transmission electron microscopy (TEM) was used to know the morphology of the particles and their size, the equipment employed was a JEOL JEM-1230 at an accelerating voltage of 120 kV. The samples were prepared by placing a drop of the original dispersion obtained on polymer-coated copper grids. The ZnO particles were analyzed by X-ray diffraction (XRD) performed on a GBC MMA SPELLMAN. Considering the diffractogram obtained, the Rietveld refinement analysis was carried out using the MAUD program (Material Analysis Using Diffraction).

2.3 Preparation of the paints

Waterborne acrylic paints were prepared in a high-speed disperser. Paint without biocides (control), which was labeled as PC, was prepared following the corresponding composition, % by weight: 26.5% styrene acrylate, 37.7% distilled water (DW), 0.2% thickener, 0.2% defoamer, 0.04% pH-stabilizer agent, 0.30% dispersant and surfactant agents, 10.0% titanium dioxide, 2.0%

precipitated calcium carbonate, 22.2% natural calcium carbonate and 0.9% coalescent agents. Also following this formulation, paints with the ZnO particles were prepared replacing, by weight, part of the natural calcium carbonate by the corresponding additive. In this sense, a paint with 1 wt% of the ZnO particles (labeled as PZnO) was prepared for the field study.

2.4 Photoactivity tests

The UV radiation effect on the additive added paints was assessed by decolorization of rhodamine-B (RB) dye under UV-A and C lamps (Philips). The UV-A lamp has a bandwidth spectrum of 315-380 nm while the UV-C lamps found within 100-280 nm range and their main emission are at 254 nm. Paints with different concentrations of ZnO (0.0, 0.12, 0.25, 0.5 and 1.0 % by weight) as additive were prepared to assess the effect of the exposition to UV lamps in laboratory conditions. Painted glass slides were stained with RB water solution (0.07 g/100 mL, 0.2 mL of solution per specimen) covering half of each sample using a pipette. After 24 h of drying, the samples were exposed to the corresponding lamps. Two specimens were analyzed for each paint, chromatic measurements (four control points for each sample surface) before UV irradiation and after 0.5, 1, 2, 4, 6, 8, 14, 20 and 26 h of exposure were performed. Due to the red color of RB, chromatic magenta-bluegreen (a^*) parameter was used to evaluate the photoactivity of stain paints [26]. In addition, change of color and gloss was determined on unstained samples.

2.5 Paints characterization

Water absorption (expressed in wt%) and water permeability (mg/cm^2) of prepared paints were determined according to ASTM D570. FTIR spectra KBr disk method was carried out using a Perkin-Elmer Spectrum One Spectrometer. Color and gloss were also determined on dried paint films employing a ByK Gardner gloss-meter. CIElab parameters were used: L^* varies from 0 to 100 (white), magenta-bluegreen (a^*) and yellow-blue (b^*) [27]. Considering these parameters, the change of color (ΔE) due to the incorporation of the ZnO particles was calculated as:

$$\Delta E = \sqrt{(L_z - L)^2 + (a_z - a)^2 + (b_z - b)^2}$$

where L_z , a_z and b_z are the parameters for the paints with ZnO and L , a and b those for the control paint. Four measurements were carried out on the panels.

2.6 Natural weathering: long-term field study

Paint films were exposed to the natural weather conditions of La Plata city (34°54'S and 57°55'W) during a period of four years. Paints were applied on masonry slabs following the guidelines of standard ASTM D 3456. The slabs were prepared in rectangular shape to obtain a test area of 315 cm² using a commercial mix. The paints were applied by brush and cured for two weeks. Finally, slabs were placed on the roof of the CIDEPINT (Experimental Station) facing north and south with an inclination of 45°. Three samples of each paint were placed for each orientation. Weathering data, such as temperatures (maximum, minimum and mean), relative humidity, solar radiation, number of rainy days, amount of falling rain and wind speed were collected during the exposure. The temperature of the panels was measured employing an infrared gun (IND 1880 INSTRU) and compared with the ambient temperature. FTIR of the films were performed to evaluate the effect of aging on the structural and functional variations of the coating. An in-depth analysis of the FTIR spectra in order to clarify the aging process was carried out by the deconvolution of the regions between 1800-1600 and 1600-1300 cm⁻¹ which allowed studying the evolution of the carbonyl and carboxylate groups. Deconvolution was carried out employing the Fit-multipeaks tool of Origin 6.0 software, with gaussians curves with adjustment of $R^2 \geq 0.98$.

At the end of the trial, contact angle, color and gloss were determined. Contact angle was obtained by drop method which was based on placing a drop of distilled water on the surface from a Pasteur pipette. The angle formed between the drop and the surface observed with a Gaosuo digital microscope was measured using Gaosuo software [28]. The procedure was repeated four times for each sample.

2.7 Biodeterioration Assessment

The resistance to biodeterioration of the paint films was assessed. Biodeterioration observed on the coatings was evaluated considering ASTM D 5590 standard which states rating (R) in relation to the percentage of the covered area: 0 (0%), 1 (<10%), 2 (10-30%), 3 (30-60%) and 4 (60-100%). Photographic records were obtained, observations were performed by stereomicroscope and scanning electron microscopy (SEM).

The mycobiota of the samples (PC and PZnO with north and south orientation) was studied after 4 years of exposition to natural weathering. The paints were rubbed with a swab and subsequently, the swabs were placed in a tube containing 2 mL of physiological solution (0.85 g of NaCl/100 mL of sterile distilled water). In Petri dishes containing Malt extract agar with streptomycin (30 mg/100 mL), 100 μ L of the stock solution were inoculated. The Petri dishes were kept at 28 °C for 10 days and filamentous fungi were isolated after 7 days following conventional

microbiological techniques [29]. The isolates were identified according to the lowest possible taxon based on their reproductive, somatic structures using standard taxonomic keys. For this, parts of mycelium were taken from mature colonies and observed under light microscope. In addition, relative density (RD) [30] and apparition relative frequency (RF) [31] of the isolate were calculated using formula (1) and (2).

$$RD(\%) = (a/b) \times 100 \quad (1)$$

where a is Number of the taxon colonies, b is Total of taxa colonies

$$RF(\%) = (c/d) \times 100 \quad (2)$$

where c is times a taxon is detected, d is Total number of sampling performed

2.8. Statistical analysis

Statistical analysis to determine the relationship between certain variables with the samples was performed using Principal Component Analysis (PCA). The packages MASS, ggplot2, scales and factoextra of the RStudio 2021.09.1® program were used to carry out the test.

3. RESULTS AND DISCUSSION

3.1 Characterization of the ZnO particles

The UV-VIS spectrum in Figure 1a shows an absorption band between 300-400nm corresponding to that reported for the surface plasmon resonance of ZnO NPs with a maximum absorption ~ 370 nm [32]. The XRD diffractogram in Figure 1b presents the representative peaks of the wurtzite crystal structure. The main diffraction planes found in order of intensity were (101), (002), (100), (110), (103), (112) and (102). Considering the diffractogram obtained and with the help of the Powder Diffraction File (PDF) files, the identification of the material was possible, but it was necessary to know more properties about it, such as particle size and network parameters. Therefore, MAUD program was used since it allows the Rietveld refinement of the structure. This program allowed carrying out a quantitative analysis of the samples, based on the diffractogram obtained from XRD and using a series of theoretical curves with which an adjustment could be carried out allowing us to know different parameters. The results of the Rietveld refinement indicate a crystal size of 23.6 nm, and the values of the lattice parameters corresponding to hexagonal zincite are: $a = 3.2495 \text{ \AA}$ and $c = 5.2089 \text{ \AA}$.

TEM micrograph in Figure 1d confirms the presence of nano-sized particles that were observed mostly grouped. Figure 1e shows the average (non-crystal) particle size by DLS was $> 100 \text{ nm}$, which

is due to the tendency of ZnO particles to gather, and this was also observed in TEM micrographs. According to XRD, DLS and TEM analyses, the synthesized ZnO particles are small aggregates (larger than 100 nm) of crystallites of an average size of 20 nm. Finally, the particles ZP resulted negative.

3.2 Photoactivity tests

The UV radiation effect on paint films with different concentration of ZnO (0, 0.125, 0.25, 0.5, 1.0 % by weight) were assessed by the decolorization of RB dye. In Figure 2a, the change in color parameter a^* of the panels exposed to the UV-A lamp can be seen. Initial a^* values were 10.7 to the blank (without ZnO) and ~ 13 for those with the nano-additive added; in general, they increased up to 8 hours. Afterwards, the values were almost constant to the coatings with ZnO. The highest one increased in a^* values corresponding to the blank which would be indicating that the presence of the nano-additive partially degraded RB, preventing the increase in magenta color.

In the case of the panels with RB exposed to UV-C lamp, Figure 2b, a^* values increased (they moved towards more positive, magenta, values) during the first hours of exposure but then, they diminished continuously, being the paint with 1% of the ZnO the one that presented the highest change in this parameter. Discoloration (decrease of a^*) due to the degradation of RB in the blank is attributed to the radiation. In Figure 2c, it can be seen photographic record of the stained samples before and after 26h facing UV-C lamp radiation with the corresponding discoloration. In the same Figure, it is presented the change of a^* ($\Delta a^* = a^*_{0h} - a^*_{26h}$) related to the concentration of ZnO. The Δa^* proved to be directly proportional to the wt% of ZnO in the coatings which is attributable to the photoactivity resulting from the corresponding particles. Due to the characteristic UV absorption of the ZnO particles with a wide band between 250 and 400 nm that can be seen in Figure 1a, the photoactive property was corroborated when the samples were exposed to UV-lamps, especially to the UV-C one, even in concentrations lower than the maximum tested.

3.3 Paint characterization

Control paint (PC) and paint with 1% of the ZnO particles (PZnO) were selected to be exposed to natural weathering considering the photoactivity tests. These paints were previously characterized. The water absorption was 17 ± 1 % to PC and 13 ± 1 % to PZnO. The decrease in water absorption when ZnO was added can be related with a better ordering of the system where smaller particles could be occupying spaces between pigment particles of greater size [33].

Permeability after 48 and 72h in contact with water resulted in a similar rate compared to the first 24 h. In this sense, 8 and 10 mg/cm² to PC and PZnO were determined, respectively.

FTIR spectra of the PC and PZnO can be examined in Figure 3. The band in the 3600–3100cm⁻¹ region is associated with OH groups present in the acrylic resin. In the case of the PC, a wider and more intense band can be observed which would be related to the molecules of water adsorbed onto the surface material. This is consistent with the higher water absorption determined in the case of the control paint with respect to the PZnO. The carbonyl band of the acrylic resin can be seen in both cases at ~ 1730 cm⁻¹ as well as the peaks at 1442, 880 and 730 cm⁻¹ corresponding to the calcium carbonate. The paint with ZnO presents a band ~ 650cm⁻¹ which could represent the inter-atomic vibrations of Zn–O bond [34]. In this spectrum, two other peaks appear at 1064 and 962cm⁻¹ which could be related to the capping agent (PVP) and their nitrated heterocycle structure.

The addition of the ZnO particles to the paint produced a change in color, $\Delta E=2.5$, rated as evident [20]. The main changes are due to the variation of the L* towards higher values and b* to more positive (yellow) ones. The gloss is also slightly increased in PZnO (5.5±0.7) related to PC (5.0 ± 0.3).

3.4 Natural weathering: long-term field study

The PC and PZnO were exposed in the CIDEPINT experimental station, which was previously described. The weather conditions in the CIDEPINT outdoor station such as: maximum, minimum temperatures, relative humidity (%) and amount of falling rain were collected and can be seen in Figure 1 of the supplementary material. The direction, frequency and speed of the winds were also collected. According to the data obtained, between May and August, the lowest temperatures were recorded at the same time with frequent rainfalls along with the lowest values of solar radiation. These facts favor the permanence of the water in contact with the material which could accelerate deterioration of the film and can lead to premature failures such as loss of adhesion and blistering. Moreover, the water content in the material is a key factor in the first constitutive stage of biofilms for both fungi and bacteria [16,35]. On the other hand, the frequency of the wind is higher in the south orientation which could be linked to a more pronounced erosive effect on samples facing south.

Temperature of the panels together with the radiation and the outdoor temperature were recorded and can be seen in Figure 4. These data show that there is an important difference in the temperature of the panels according to the orientation, generally, higher when they are facing north. In this case, it is also important the difference between the outdoor temperature and the temperature

of the panels, being 10-12°C when the solar radiation is high ($>800 \text{ Wm}^{-1}$). This proves that solar radiation is higher on the samples facing north.

FTIR spectra of the paint films facing north and south after a year and a half are shown in Figure 5. The band at 3600–3100 cm^{-1} , associated with OH groups, was present in all samples. PC facing south showed the broadest band compared to the others, Figure 5a. This could be attributed to the adsorption of water on the surface of the film [36]. The same band can be seen from the paints with ZnO particles, in Figure 5b, but with less width than in the case of the PC samples. Peaks corresponding to carbonyl ($\sim 1730 \text{ cm}^{-1}$) and carboxylate ($\sim 1442 \text{ cm}^{-1}$) groups show greater intensity in samples after natural weathering with both PC and PZnO and for both orientations. This was corroborated by the deconvolution analysis, resulting from the areas corresponding to the carbonyl group before natural weathering of 231 and 375 to the PC and PZnO, while to the carboxylate group were 586 and 1130, respectively. After the exposition, the areas corresponding to the carbonyl group increased to 578 (PC north), 558 (PC south), 444 (PZnO north) and 648 (PZnO south) while those corresponding to the carboxylate group increased to 2174, 1210, 1130, 1229 and 1853, respectively. The carbonyl groups growth for aged samples can be related to the formation of the oxidation products such as carboxylic acids, aldehydes and ketones [37]. PZnO facing north presented the lowest intensity related to these peaks. Taking into account that in the south hemisphere panels facing north received more solar radiation, the opposite could be expected. Therefore, the lowest intensity of the peaks corresponding to the carbonyl and carboxylate groups for the samples exposed to the north can be attributed to the volatilization of small molecules as proposed by Chiantore *et al.*, due to chain scissions by photolysis and photooxidative process of acrylic polymers [38]. Moreover, the backbone structure presented the same trend as the peaks corresponding to C-H stretching, 3000–2800 cm^{-1} . According to this, photooxidative degradation would be favored in the samples oriented to the north where solar radiation has been reported as higher. In that sense, the higher photoactivity evidenced in the PZnO facing north can be related to the self-cleaning mechanism and its antimicrobial effect.

It is known that the UV-shielding effect of ZnO particles is attributed to the absorption in the UV spectrum but, at the same time, this allows that the electrons from the forbidden band can jump into the conduction band resulting in the generation of electron–hole pairs [24]. These positive holes and negative electrons can react with water, oxygen molecules or hydroxyl groups on the surface of the particles leading to the formation of free radicals that might degrade the binder polymer [39]. It has been reported that acrylic coatings increase the absorption of UV-light by increasing the concentration of the ZnO NPs in the paint which seems to be accentuated for concentrations $\geq 2 \text{ wt}\%$

in short-term studies performed in UV weathering chambers and laboratory [8,39]. The size of the particles has been studied as another factor, in this sense, smaller nano particles < 30 nm have been associated to polymer degradation [3]. Therefore, even though in the present research, certain degradation of the binder is observed from the analysis of the FTIR spectra, this did not compromise the integrity of the paint films with ZnO particles as it could be seen in the inspections and in the stereomicroscope observations. This is consistent with the bibliographic data that indicates the advantages of using concentrations below 2 wt% and larger particles which would be counteracting the photodegrading effect of the ZnO particles [40].

The contact angle determined for the paint films before and after four years showed an increase after natural weathering for the PZnO from $50 \pm 2^\circ$ to $63 \pm 2^\circ$ for samples facing north and to $60 \pm 2^\circ$ for those facing south. While the PC samples presented no significant changes and registered a contact angle before exposition of $47 \pm 4^\circ$ and after facing north and south orientations $43 \pm 6^\circ$ and $50 \pm 2^\circ$, respectively. PZnO facing north resulted in the highest contact angle showing higher surface hydrophobicity which agrees with the results observed in the FTIR.

The change of color (ΔE) after four years resulted important for all the paints (PC and PZnO) facing south and north: 10.8, 10.4, 9.4 and 9.7, respectively. The main changes are due to the variation of b^* to more positive values (yellow). The gloss decreased in all cases to 1.4 ± 0.1 for the PC samples (south), PZnO (south) and PZnO (north) and in the case of PC (north) to 1.3 ± 0.1 .

3.5 Biodeterioration assessment

Paints exposed to natural weathering were evaluated related to their biodeterioration. In order to rate the performance in each case, visual inspection was carried out. Photographic records of representative samples obtained over four years are shown in Figure 2 of the supplementary material. PC samples showed the first signs of biodeterioration after the first year of exposition (R=2), unlike the PZnO where trace of growth (R=1) was present. Until then, no differences could be appreciated between PZnO facing north and south. In Figure 6, images obtained by stereomicroscope are shown and it can be seen the degree of development of the biofilm with dark colored filamentous structures deployed radially which is a characteristic of filamentous fungi in PC samples. This was corroborated by SEM observations of the samples (images not shown).

After three years, the controls showed an increase of spoilage (R = 3) and the development of lichens could be directly appreciated on the films in both north and south orientations. No major changes were observed in the paint films facing north with ZnO particles being R=1 while, in the panels facing south, the appearance of a few isolated lichens with little development were observed.

In Figure 6, it can be seen in more detail how the biofilm spreads over a larger area of the PC film and the biodegradation was more evident because the support material can be seen in some parts thanks to the higher magnification of the stereomicroscope (80x).

At the end of the test (fourth year), the area covered by biofilm increased in the PC samples in both north and south (R=4) observing more lichens in the north orientation. The PZnO samples maintained a significant difference with the control samples with trace to light biofilm growth (R=1-2) being PZnO samples facing north those with the better performance as it can be seen in Figure 2 of the supplementary material.

The possible mechanisms of the paint biodegradation (without nano-additive) could be explained considering that the microorganisms in the biofilm secrete enzymes such as lipases and oxidases that catalyze the hydrolysis of the ester groups and C-C backbone cleavage in the acrylic polymer (resin), respectively [41,42]. On the other hand, the release of different metabolites (e.g. organic acids, phenolic compounds, amino acids, siderophores, protons, etc.) facilitate the mobilization of metals from the pigments (CaCO_3 and TiO_2) in the film [43,44]. In addition to the mechanisms of chemical biodegradation, there is also invasive growth by filamentous fungi that, through their hyphae, penetrate the material on which they grow. These biodegradation mechanisms are shown in Figure 7a.

The presence of the ZnO nano-crystallites in the paint would be interfering with the biodegradation mechanisms presented due to the fact that, under UV irradiation on their surface, they produce oxygenated radicals that come into contact with cell membranes as it can be seen in Figure 7b [45]. These reactive oxygen species (ROS) disrupt the membranes and interfere with DNA and protein functions which can lead to cell death [45]. Although it was observed through the FTIR spectra analysis results that the presence of the ZnO affected the acrylic resin, in the long term, the antimicrobial and self-cleaning photoactive surface effect appeared to be more relevant to the integrity of the coating. The establishment of biofilms on the surface of the PC films and the deployment of a true degradation system constituted by enzymes, organic acids, among other metabolites, and the invasive growth, generate a deeper damage in the material. In this sense, the invasive growth of fungi breaks through the surface line of the material while the activity displayed by the ZnO nano-crystallites occurs at surface level in the interface of the material with the environment where UV light is incident.

The PZnO films maintained integrity after four years, unlike the PC samples, being better the performance of those facing north which could be related with the higher solar radiation in this orientation. Chai et al. suggested that a maximum admissible degradation limit of 20-30% is the most

adequate value to establish the end of the service life of the painted façades [46]. Considering this and the results obtained, the service life of the control paints (without biocide) facing both orientations was compromised around a year and a half of the exposition. PC samples were rated as 2 with biodeterioration signs in a 20-30% of the surface. Therefore, the incorporation of the ZnO proved to extend the service life of the formulated paint.

On the other hand, from the microbiological evaluation of the samples, it was possible to study the cultivable mycobiota associated with the samples at the fourth year. The isolates were the same for each sample but the paints facing south presented higher RF of appearance and RD in comparison with the samples facing north. For example, on PC samples with south orientation, the RF of the isolated was *Rhodotorula* sp. (95%), *Cladosporium* sp. (90%), *Alternaria* sp. (75%), *Epicoccum nigrum* (69%) and *Mucor* sp. (55%). However, these same strains in PC with north orientation had a RF of 85, 80, 70, 65 and 50 % respectively. Taking into account, what was proposed by Esquivel et al., from RF values of the fungi, the following ecological categories were given: abundant (81–100%); common (61–80%); moderate (41–60%); occasional (21–40%); and rare (0.1–20%). Therefore, *Rhodotorula* sp. (Basidiomycota) and *Cladosporium* sp. (Ascomycota) are abundant; *Alternaria* sp. (Ascomycota) and *Epicoccum nigrum* (Ascomycota) are common and *Mucor* sp. (Mucoromycota) is moderate [31].

In addition, regardless of the sample orientation, in the PZnO samples, fungi had lower RF and RD than PC samples. Also, regarding the strains previously mentioned, *Penicillium* sp. was isolated only from the PZnO. Other authors reported these species related to the city of La Plata. For example, it has been reported the presence of *Cladosporium* sp., *Alternaria* sp., *Penicillium* sp. and *Mucor* sp. in CIDEPINT (Experimental Station) with RF of appearance similar to the one described in the present work [29]. In addition, *Rhodotorula* sp. was found as part of the microbiofouling of crypts of historical and architectural interest at La Plata Cemetery [47].

Environmental conditions may also influence the mycobiota present in the samples and are strongly governed by geographical location and seasonality. Temperature, relative humidity, solar radiation, number of rainy days, amount of falling rain and wind speed are abiotic factors that determine species prevalence during the period of 4 years of study. The effect of each factor varies according to fungal species, with their complex not fully understood dynamics. For example, temperature and water availability will affect the size of the fungal source and will control the active release of some fungal spores [48]. *Cladosporium* sp., *Alternaria* sp. and *Penicillium*, are very frequently found and have a wide growth range at different relative humidity values and temperatures [49]. Therefore, in a place with an annual average temperature of 18 ± 1 °C and a relative humidity

of 77 ± 3 %, the presence of these species is favored. On the other hand, *Epicoccum nigrum* is considered a typical colonizer in decaying vegetation [50], then wind speeds of 12.3 ± 0.8 Km/h can promote the airborne transport of fungal propagules from local vegetation sources. Finally, naturally pigmented yeasts may well produce carotenoids, as in the case of *Rhodotorula* sp., that ensure their survival in extreme environments with average solar radiation of 614 Wm^{-1} .

On the other hand, PCA was employed to explore the samples based on certain variables using RStudio 2021.09.1® program, whose axes explained 95% of variation. Figure 8 shows PCA ordination of samples according to the variables analyzed. Axis 1 shows average temperature and ΔE with 56.9 % of variation and axis 2 shows that 38.2% corresponded to the biodeteriorating rating, RF, RD, contact angle and gloss. An exploratory PCA revealed that there is no clustering between the samples and that PC (North), and PC (South) have higher values of biodeterioration rating, RF and RD, possibly due to the absence of ZnO particles in the formulation and the difference in orientation.

4. CONCLUSION

The ZnO particles were synthesized by an ecofriendly precipitation method. The nanometric ZnO crystallites (~ 20 nm) presented a wide absorption band in the UV spectrum. The nano-additive was integrated in the preparation of acrylic paints and the photoactivity was corroborated. Paint without any biocide and paint with 1 wt% of the ZnO particles were exposed to natural weathering in a long-term field study. The paints films with ZnO facing north were the most efficient for biodeterioration control after four years of exposition. Due to temperatures, rainfalls, and solar radiation, the months between May and August were those that favored the permanence of water in the material which would facilitate the development of biofilms. The solar radiation was higher in samples facing north which would allow greater photoactivity by the ZnO particles in the paint film. The aged paint films showed through the FTIR spectra an increase in oxidation in all samples and evidenced the photoactivity of PZnO facing north, corroborating a higher antimicrobial activity exhibited by these samples. The PC samples facing north presented after three years a larger surface area with biodeterioration where many lichens compromised the integrity of the films as it could be corroborated by stereomicroscope observations. Therefore, it was shown that the photoactivity of ZnO ends up benefiting the integrity of the film in the long term. In this sense, once an extension $\sim 30\%$ of the surface of the PC film is covered by biofilm (between 1 and 2 years) its integrity will be deeply compromised due to the deployment of a complex degradation system that acts at a

chemical and physical level. Finally, the incorporation of the ZnO particles proved to extend the service life of the formulated paints.

5. ACKNOWLEDGEMENTS

The authors are grateful to Consejo Nacional de Investigaciones Científicas y Técnicas (CONICET), Comisión de Investigaciones Científicas de la Provincia de Buenos Aires (CICPBA), Agencia Nacional de Promoción Científica y Tecnológica (ANPCyT) and to Universidad Nacional de La Plata (UNLP), Ministerio de Ciencia, Tecnología e Innovación Productiva for sponsoring this research work. This study was partially supported by the Consejo Nacional de Ciencia y Tecnología (CONACyT). The authors thank to Departamento de Sismología e Información Meteorológica from the Facultad de Ciencias Astronómicas y Geofísicas, Universidad Nacional de La Plata for providing the weathering data of La Plata city. They especially thank to the CIDEPINT service sector (Ing. Mateo Paez and Diego Tunessi) and the technical support of: Eng. Pablo Bellotti and Lic. Claudio Cerruti. Finally, thanks for the collaboration of Sergio F. Rojas and Leonardo Rojas.

6. REFERENCES

- [1] S.M. Somtürk, I.Y. Emek, S. Senler, M. Eren, S.Z. Kurt, M. Orbay, Effect of wollastonite extender on the properties of exterior acrylic paints, *Prog. Org. Coatings*. 93 (2016) 34–40. doi:10.1016/j.porgcoat.2015.12.014.
- [2] A.C.F. Tornero, M.G. Blasco, M.C. Azqueta, C.F. Acevedo, C.S. Castro, S.J.R. López, Antimicrobial ecological waterborne paint based on novel hybrid nanoparticles of zinc oxide partially coated with silver, *Prog. Org. Coatings*. 121 (2018) 130–141. doi:10.1016/j.porgcoat.2018.04.018.
- [3] M. Eren, H.K. Can, Preparation of zinc methacrylate-methylmethacrylate-butyl acrylate emulsions and their application in exterior paints, *Prog. Org. Coatings*. 135 (2019) 424–437. doi:10.1016/j.porgcoat.2019.06.031.
- [4] C. Gaylarde, A. Otlewska, S. Celikkol-Aydin, J. Skóra, M. Sulyok, K. Pielech-Przybylska, J. Gillatt, I. Beech, B. Gutarowska, Interactions between fungi of standard paint test method BS3900, *Int. Biodeterior. Biodegradation*. 104 (2015) 411–418. doi:10.1016/j.ibiod.2015.07.010.
- [5] A. Rauf, R.H. Crawford, Building service life and its effect on the life cycle embodied energy of buildings, *Energy*. 79 (2015) 140–148. doi:10.1016/j.energy.2014.10.093.
- [6] A. Silva, J. de Brito, Service life of building envelopes: A critical literature review, *J. Build. Eng.* 44 (2021) 102646. doi:10.1016/j.job.2021.102646.
- [7] V.K. Konaganti, G. Madras, Photooxidative and pyrolytic degradation of methyl

- methacrylate-alkyl acrylate copolymers, *Polym. Degrad. Stab.* 94 (2009) 1325–1335. doi:10.1016/j.polymdegradstab.2009.06.003.
- [8] M. Baudys, J. Krýsa, M. Zlámal, A. Mills, Weathering tests of photocatalytic facade paints containing ZnO and TiO₂, *Chem. Eng. J.* 261 (2015) 83–87. doi:10.1016/j.cej.2014.03.112.
- [9] K. Bester, X. Lamani, Determination of biocides as well as some biocide metabolites from facade run-off waters by solid phase extraction and high performance liquid chromatographic separation and tandem mass spectrometry detection, *J. Chromatogr. A.* 1217 (2010) 5204–5214. doi:10.1016/j.chroma.2010.06.020.
- [10] C. Paijens, A. Bressy, B. Frère, R. Moillon, Biocide emissions from building materials during wet weather: identification of substances, mechanism of release and transfer to the aquatic environment, *Environ. Sci. Pollut. Res.* 27 (2020) 3768–3791. doi:10.1007/s11356-019-06608-7.
- [11] P. Vega-Garcia, R. Schwerd, C. Scherer, C. Schwitalla, S. Johann, S.H. Rommel, B. Helmreich, Influence of façade orientation on the leaching of biocides from building façades covered with mortars and plasters, *Sci. Total Environ.* 734 (2020) 139465. doi:10.1016/j.scitotenv.2020.139465.
- [12] M.A. Kakakhel, F. Wu, J.D. Gu, H. Feng, K. Shah, W. Wang, Controlling biodeterioration of cultural heritage objects with biocides: A review, *Int. Biodeterior. Biodegrad.* 143 (2019). doi:10.1016/j.ibiod.2019.104721.
- [13] A. Chaudhuri, S. Bhattacharyya, P. Chaudhuri, M. Sudarshan, S. Mukherjee, In vitro deterioration study of concrete and marble by *Aspergillus tamarii*, *J. Build. Eng.* 32 (2020). doi:10.1016/j.jobbe.2020.101774.
- [14] G.M. Gadd, Y.J. Rhee, K. Stephenson, Z. Wei, Geomycology: Metals, actinides and biominerals, *Environ. Microbiol. Rep.* 4 (2012) 270–296. doi:10.1111/j.1758-2229.2011.00283.x.
- [15] M. Gambino, M.A.A.A. Ahmed, F. Villa, F. Cappitelli, Zinc oxide nanoparticles hinder fungal biofilm development in an ancient Egyptian tomb, *Int. Biodeterior. Biodegrad.* 122 (2017) 92–99. doi:10.1016/j.ibiod.2017.05.011.
- [16] O.C.G. Adan, R.A. Samson, *Fundamentals of mold growth in indoor environments and strategies for healthy living*, First, Wageningen Academic Publishers, The Netherlands, 2011. doi:10.3920/978-90-8686-722-6.
- [17] P. Dileep, S. Jacob, S.K. Narayanankutty, Functionalized nanosilica as an antimicrobial additive for waterborne paints, *Prog. Org. Coatings.* 142 (2020) 105574. doi:10.1016/j.porgcoat.2020.105574.
- [18] L.E. Mardones, M.S. Legnoverde, J.D. Monzón, N. Bellotti, E.I. Basaldella, Increasing the effectiveness of a liquid biocide component used in antifungal waterborne paints by its encapsulation in mesoporous silicas, *Prog. Org. Coatings.* 134 (2019) 145–152. doi:10.1016/j.porgcoat.2019.04.058.
- [19] S. Hendessi, E.B. Sevinis, S. Unal, F.C. Cebeci, Y.Z. Menciloglu, H. Unal, Antibacterial sustained-release coatings from halloysite nanotubes/waterborne polyurethanes, *Prog. Org. Coatings.* 101 (2016) 253–261. doi:10.1016/j.porgcoat.2016.09.005.
- [20] R.A. Arreche, K. Igal, N. Bellotti, C. Deyá, P.G. Vázquez, Functionalized zirconia compounds as antifungal additives for hygienic waterborne coatings, *Prog. Org. Coatings.* 128 (2019).

- doi:10.1016/j.porgcoat.2018.12.004.
- [21] S.M. Amorim, J. Suave, L. Andrade, A.M. Mendes, H.J. José, R.F.P.M. Moreira, Towards an efficient and durable self-cleaning acrylic paint containing mesoporous TiO₂ microspheres, *Prog. Org. Coatings*. 118 (2018) 48–56. doi:10.1016/j.porgcoat.2018.01.005.
- [22] C. Jayaseelan, A.A. Rahuman, A.V. Kirthi, S. Marimuthu, T. Santhoshkumar, A. Bagavan, K. Gaurav, L. Karthik, K.V.B. Rao, Novel microbial route to synthesize ZnO nanoparticles using *Aeromonas hydrophila* and their activity against pathogenic bacteria and fungi, *Spectrochim. Acta - Part A Mol. Biomol. Spectrosc.* 90 (2012) 78–84. doi:10.1016/j.saa.2012.01.006.
- [23] K. Loh, C.C. Gaylarde, M.A. Shirakawa, Photocatalytic activity of ZnO and TiO₂ ‘nanoparticles’ for use in cement mixes, *Constr. Build. Mater.* 167 (2018) 853–859. doi:10.1016/j.conbuildmat.2018.02.103.
- [24] J.G. Clar, W.E. Platten, E. Baumann, A. Remsen, S.M. Harmon, K. Rodgers, T.A. Thomas, J. Matheson, T.P. Luxton, Release and transformation of ZnO nanoparticles used in outdoor surface coatings for UV protection, *Sci. Total Environ.* 670 (2019) 78–86. doi:10.1016/j.scitotenv.2019.03.189.
- [25] L. Trotsiuk, A. Antanovich, A. Lizunova, O. Kulakovich, Direct synthesis of amphiphilic polyvinylpyrrolidone-capped gold nanoparticles in chloroform, *Colloids Interface Sci. Commun.* 37 (2020) 100289. doi:10.1016/j.colcom.2020.100289.
- [26] E. Quagliarini, F. Bondioli, G.B. Goffredo, C. Cordoni, P. Munafò, Self-cleaning and de-polluting stone surfaces: TiO₂ nanoparticles for limestone, *Constr. Build. Mater.* 37 (2012) 51–57. doi:10.1016/j.conbuildmat.2012.07.006.
- [27] L.G. Ecco, S. Rossi, M. Fedel, F. Deflorian, Color variation of electrophoretic styrene-acrylic paints under field and accelerated ultraviolet exposure, *Mater. Des.* 116 (2017) 554–564. doi:10.1016/j.matdes.2016.12.051.
- [28] E. Gámez-Espinosa, L. Barberia-Roque, O.F. Obidi, C. Deyá, N. Bellotti, Antifungal applications for nano-additives synthesized with a bio-based approach, *Adv. Nat. Sci. Nanosci. Nanotechnol.* 11 (2020) 015019. doi:10.1088/2043-6254/ab790f.
- [29] E. Gámez-Espinosa, N. Bellotti, C. Deyá, M. Cabello, Mycological studies as a tool to improve the control of building materials biodeterioration, *J. Build. Eng.* 32 (2020) 101738. doi:10.1016/j.jobbe.2020.101738.
- [30] R. Smith, *Ecology and Field Biology*, 3rd ed, Harper and Row, New York, 1980.
- [31] P. Esquivel, M. Mangiaterra, G. Giusiano, M.A. Sosa, Anemophilous microfungi in outdoor environments of two cities in Argentinian northeastern, *Boletín Micológico*. 18 (2003) 21–28. doi:10.22370/bolmicol.2003.18.0.376.
- [32] M.S. Lowry, D.R. Hubble, A.L. Wressell, M.S. Vratsanos, F.R. Pepe, C.R. Hegedus, Assessment of UV-permeability in nano-ZnO filled coatings via high throughput experimentation, *J. Coatings Technol. Res.* 5 (2008) 233–239. doi:10.1007/s11998-007-9064-6.
- [33] A. Mathiazhagan, R. Joseph, Nanotechnology-A New Prospective in Organic Coating - Review, *Int. J. Chem. Eng. Appl.* 2 (2011) 225–237. doi:10.7763/IJCEA.2011.V2.108.
- [34] D. Dodoo-Arhin, T. Asiedu, B. Agyei-Tuffour, E. Nyankson, D. Obada, J.M. Mwabora, Photocatalytic degradation of Rhodamine dyes using zinc oxide nanoparticles, *Mater. Today Proc.* (2020). doi:10.1016/j.matpr.2020.04.597.

- [35] C. Grant, C.A. Hunter, B. Flannigan, A.F. Bravery, The moisture requirements of moulds isolated from domestic dwellings, *Int. Biodeterior.* 25 (1989) 259–284. doi:10.1016/0265-3036(89)90002-X.
- [36] K. Wojciechowski, G.Z. Zukowska, I. Korczagin, P. Malanowski, Effect of TiO₂ on UV stability of polymeric binder films used in waterborne facade paints, *Prog. Org. Coatings.* 85 (2015) 123–130. doi:10.1016/j.porgcoat.2015.04.002.
- [37] M. Vlad Cristea, B. Riedl, P. Blanchet, Enhancing the performance of exterior waterborne coatings for wood by inorganic nanosized UV absorbers, *Prog. Org. Coatings.* 69 (2010) 432–441. doi:10.1016/j.porgcoat.2010.08.006.
- [38] O. Chiantore, L. Trossarelli, M. Lazzari, Photooxidative degradation of acrylic and methacrylic polymers, *Polymer (Guildf).* 41 (2000) 1657–1668. doi:10.1016/S0032-3861(99)00349-3.
- [39] T.V. Nguyen, P.H. Dao, K.L. Duong, Q.H. Duong, Q.T. Vu, A.H. Nguyen, V.P. Mac, T.L. Le, Effect of R-TiO₂ and ZnO nanoparticles on the UV-shielding efficiency of water-borne acrylic coating, *Prog. Org. Coatings.* 110 (2017) 114–121. doi:10.1016/j.porgcoat.2017.02.017.
- [40] G.G. Goourey, P. Wong-Wah-Chung, L. Balan, Y. Israëli, Effects of ZnO quantum dots on the photostability of acrylate photopolymers used as recording materials, *Polym. Degrad. Stab.* 153 (2018) 172–184. doi:10.1016/j.polymdegradstab.2018.04.026.
- [41] I. Gaytán, M. Burelo, H. Loza-Tavera, Current status on the biodegradability of acrylic polymers: microorganisms, enzymes and metabolic pathways involved, *Appl. Microbiol. Biotechnol.* 105 (2021) 991–1006. doi:10.1007/s00253-020-11073-1.
- [42] R. Bellucci, P. Cremonesi, G. Pignagnoli, Conservation : the Removal of Aged Acrylic Resin, *Stud. Conserv.* 44 (1999) 278–281.
- [43] G. Michael, J. Bahri-esfahani, Q. Li, Oxalate production by fungi: significance in geomycology, biodeterioration and bioremediation, *Fungal Biol. Rev.* 28 (2014) 36–55. doi:10.1016/j.fbr.2014.05.001.
- [44] I. Beech, A. Otlewska, J. Skóra, B. Gutarowska, C. Gaylarde, Interactions of fungi with titanium dioxide from paint coating, *Indoor Built Environ.* 27 (2018) 263–269. doi:10.1177/1420326X16670716.
- [45] Y. Li, C. Liao, S.C. Tjong, Recent advances in zinc oxide nanostructures with antimicrobial activities, *Int. J. Mol. Sci.* 21 (2020) 1–70. doi:10.3390/ijms21228836.
- [46] C. Chai, J. De Brito, P.L. Gaspar, A. Silva, Statistical modelling of the service life prediction of painted surfaces, *Int. J. Strateg. Prop. Manag.* 19 (2015) 173–185. doi:10.3846/1648715X.2015.1031853.
- [47] P.S. Guiamet, V. Rosato, S.G. de Saravia, A.M. García, D.A. Moreno, Biofouling of crypts of historical and architectural interest at La Plata Cemetery (Argentina), *J. Cult. Herit.* 13 (2012) 339–344. doi:10.1016/j.culher.2011.11.002.
- [48] A.M. Jones, R.M. Harrison, The effects of meteorological factors on atmospheric bioaerosol concentrations—a review, *Sci. Total Environ.* 326 (2004) 151–180. doi:10.1016/j.scitotenv.2003.11.021.
- [49] J.C. Samson, R.A.; Hoekstra, E.S.; Frisvad, Introduction to food and airborne fungi, 7th ed., CBS, The Netherlands, 2004.

- [50] J.I. Pitt, A.D. Hocking, *Fungi and Food Spoilage*, Springer US, Boston, MA, 2009.
doi:10.1007/978-0-387-92207-2.

Journal Pre-proof

Figures captions

Figure 1. Characterization of the ZnO particles: a) UV-VIS absorption spectrum (spike at 650 nm is an artifact coming from the spectrometer); b) XRD diffractogram; c) TEM micrographs and d) particle size distribution.

Figure 2. Photoactivity tests: a) variation in color parameter a^* over time for paint with different wt % of the ZnO particles exposed to UV-A lamp; b) variation in color parameter a^* over time for paint with different wt % of the ZnO particles exposed to UV-C lamp; c) photographic records of the samples (+ RB dye) with different wt % of the ZnO particles exposed to the UV-C lamp and the Δa^* calculated to the same samples as function of the wt % of the ZnO particles in the paint.

Figure 3. FTIR spectra of the PC and PZnO films before the exposition to the natural weathering.

Figure 4. Temperature of the samples exposed to the north and south orientations, outdoor temperature, and solar radiation.

Figure 5. FTIR spectra of the paint films before natural weathering (NW) and after exposition for 1.5 years to the north and south orientations: a) PC and b) PZnO.

Figure 6. Natural weathering: stereomicroscope images (10x and 80x) of the PC and PZnO samples after 1.5 and 3 years of exposition to the north and south orientations.

Figure 7. a) Biodegradation routes for the major components of the paint (without antimicrobial additive): Acrylic polymer (resin) [41]; CaCO_3 (pigment) [43] and TiO_2 (pigment) [44]. b) Mechanism of antimicrobial activity on the surface of the paint film with ZnO particles.

Figure 8. PCA ordering of samples according to the variables analyzed at the end of the field test (biodeterioration rate, color change ΔE , gloss, contact angle, DR, RF and average temperature of the panels).

Supplementary material

Figure 1. Weather conditions: a) maximum/minimum temperature, relative humidity, amount of falling rain and b) direction, frequency (%) and speed (km/h) mean \pm std dev, of the winds. CIDEPINT outdoor station data along the exposure time.

Figure 2. Natural weathering: photographic registers obtained during the four years study.

Figure 1

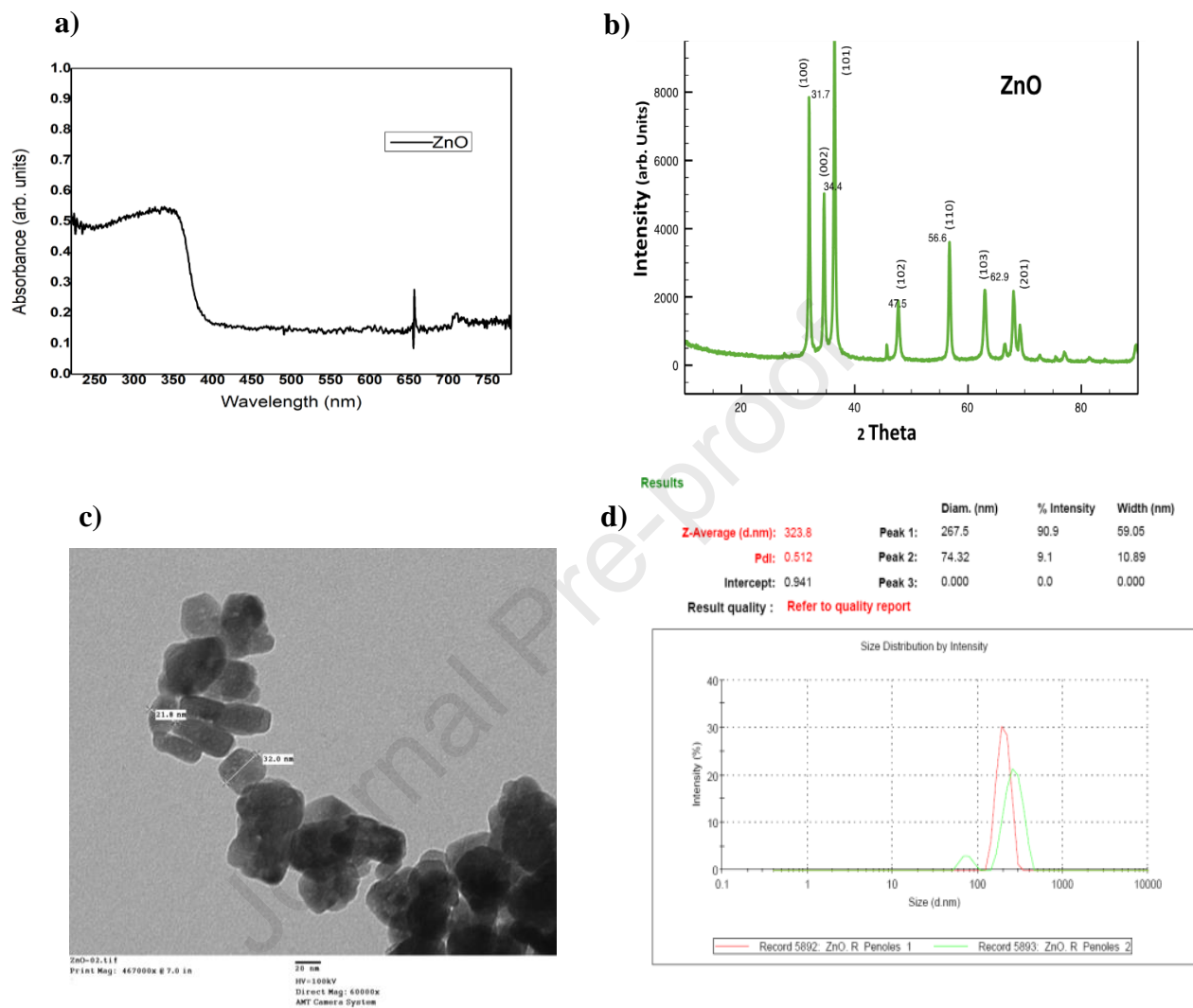


Figure 2

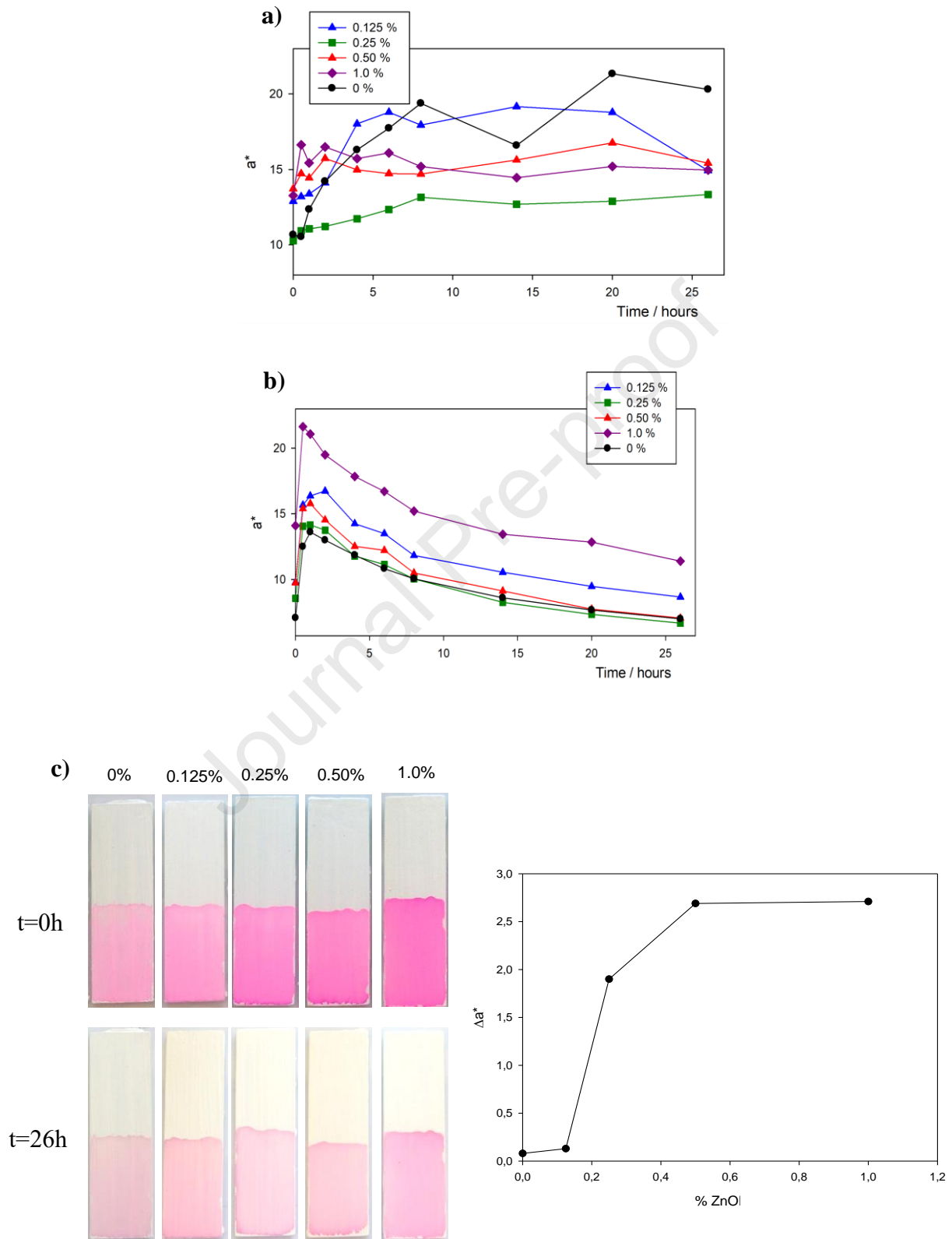


Figure 3

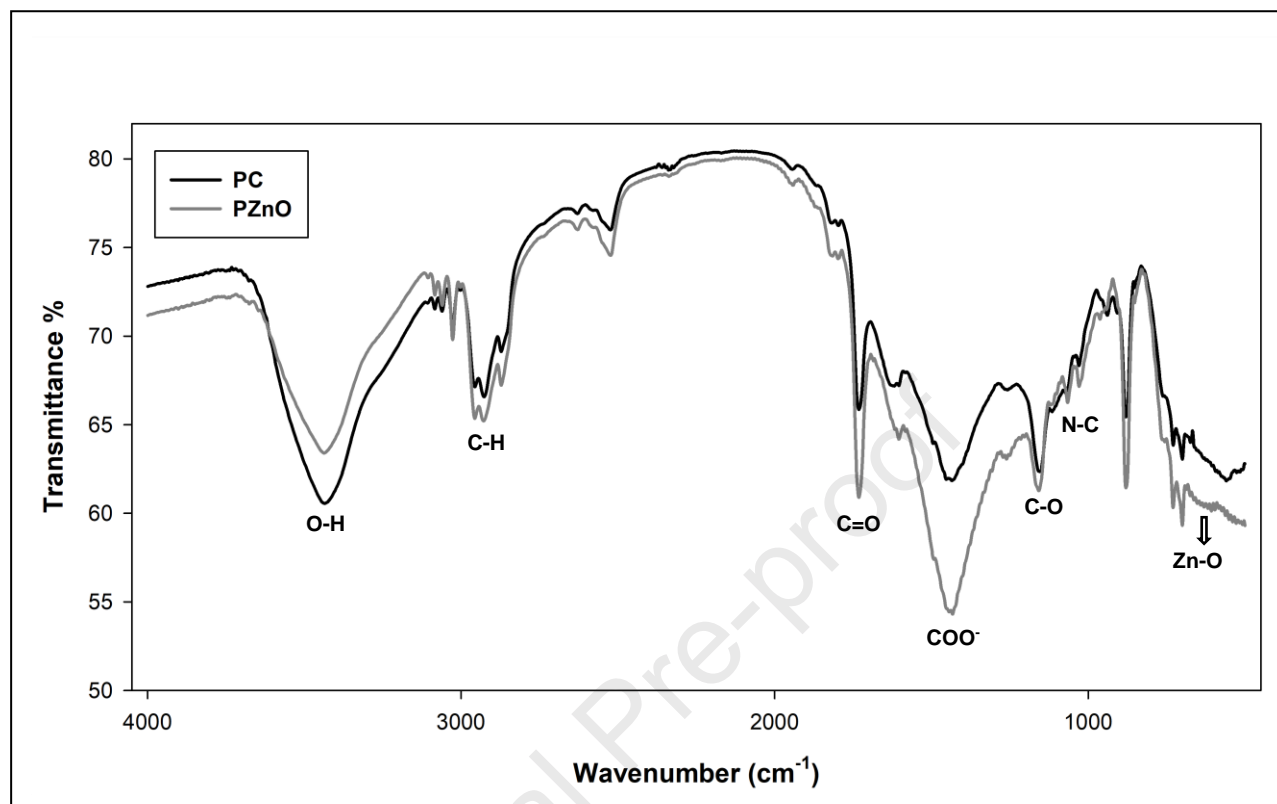


Figure 4

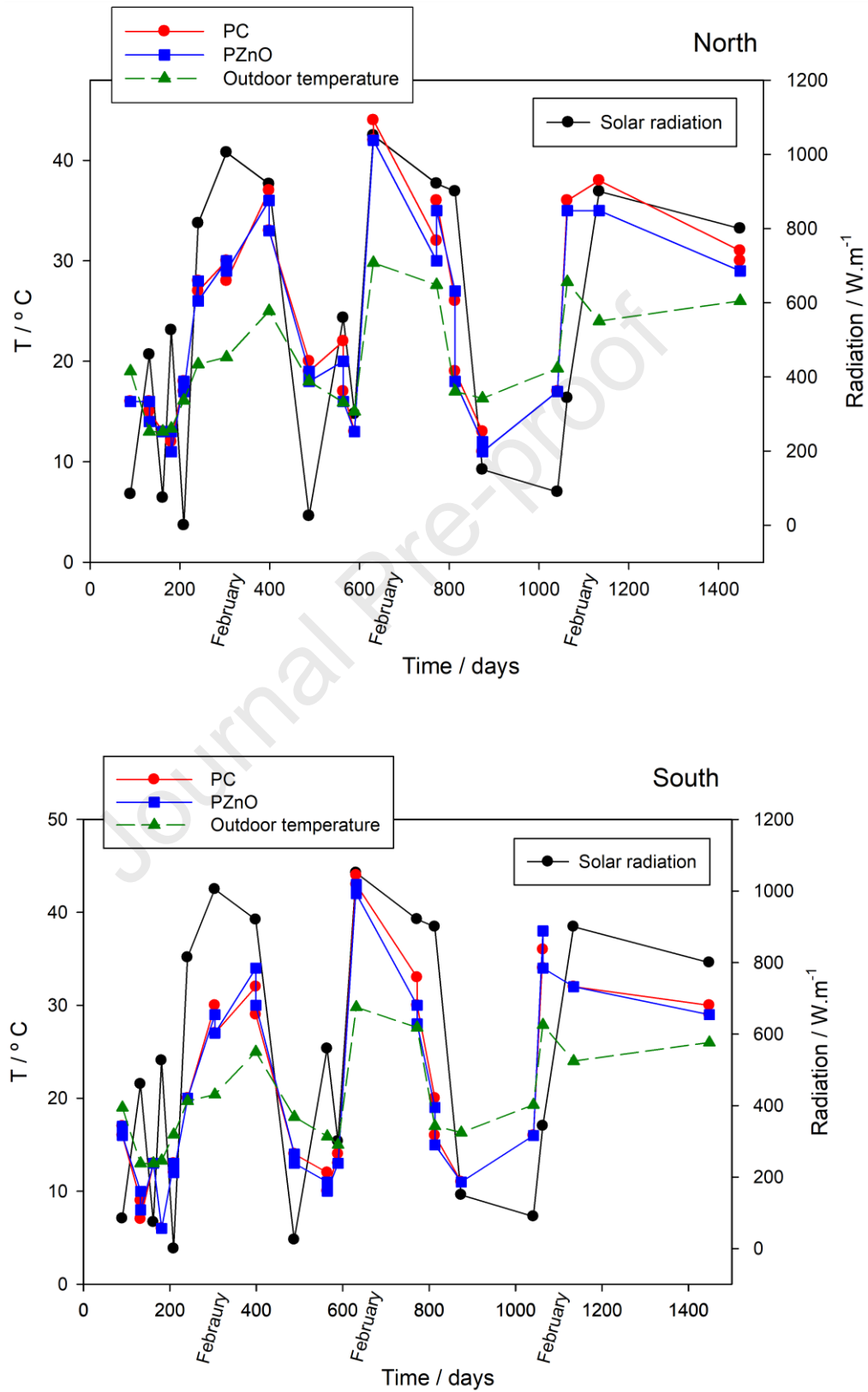
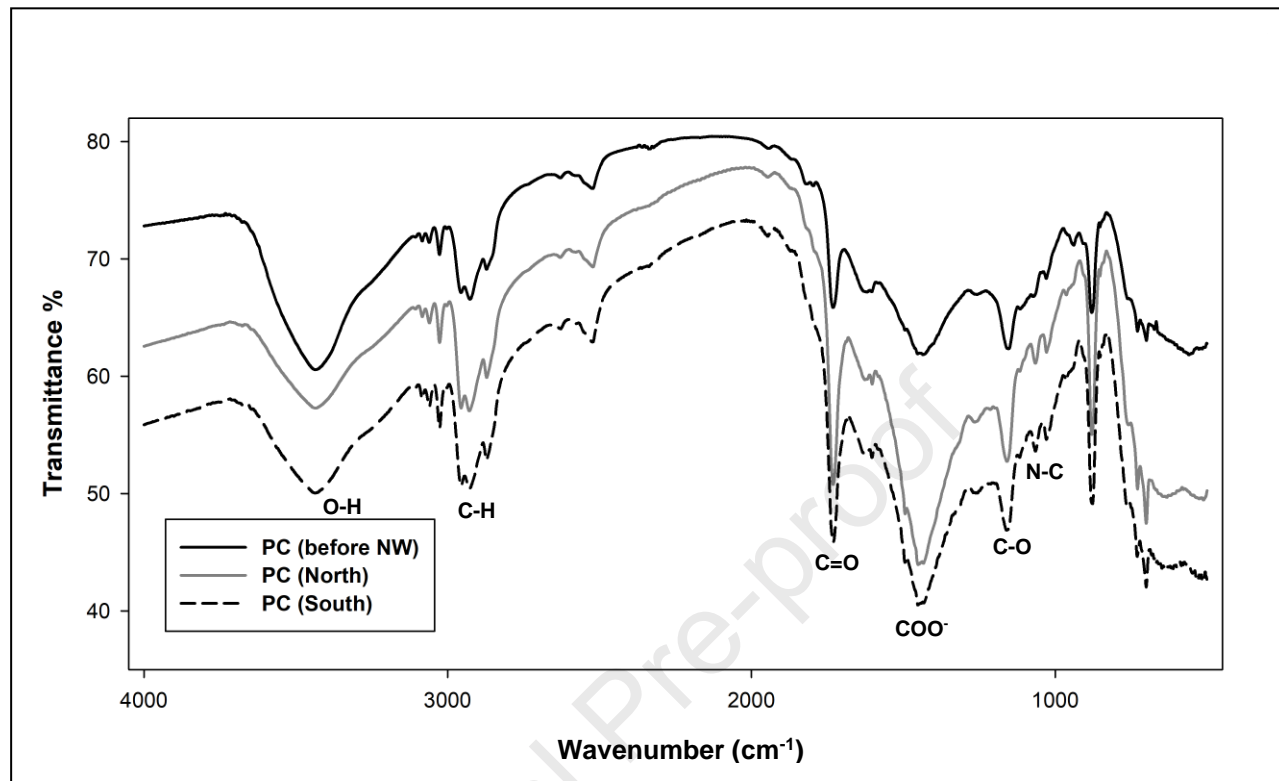


Figure 5

a)



b)

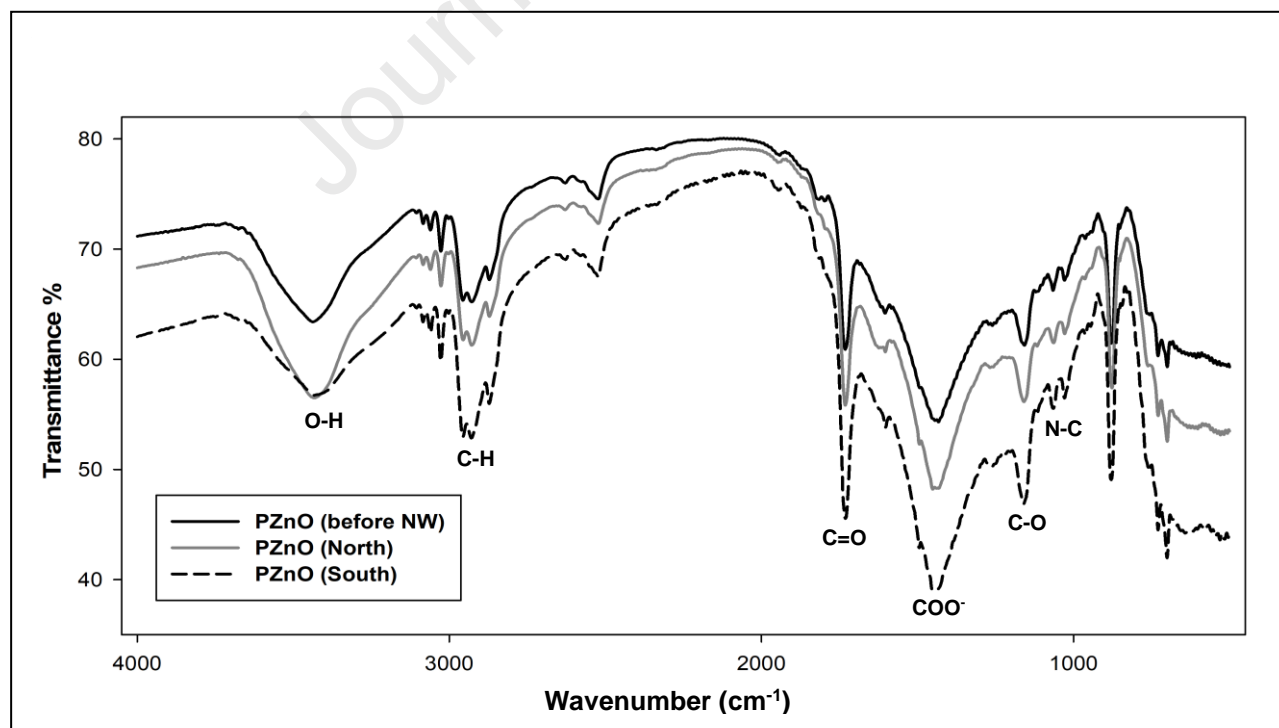


Figure 6

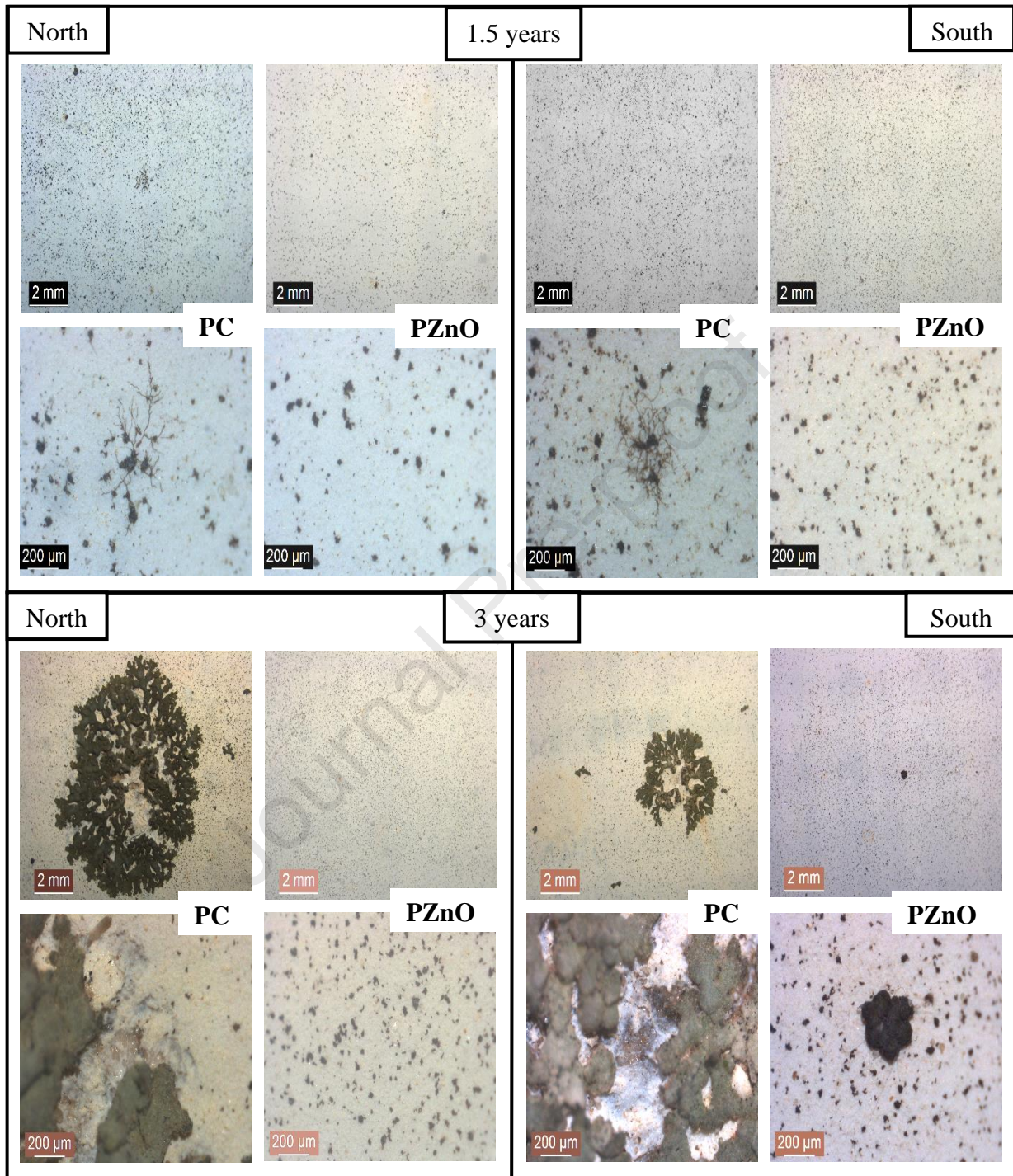
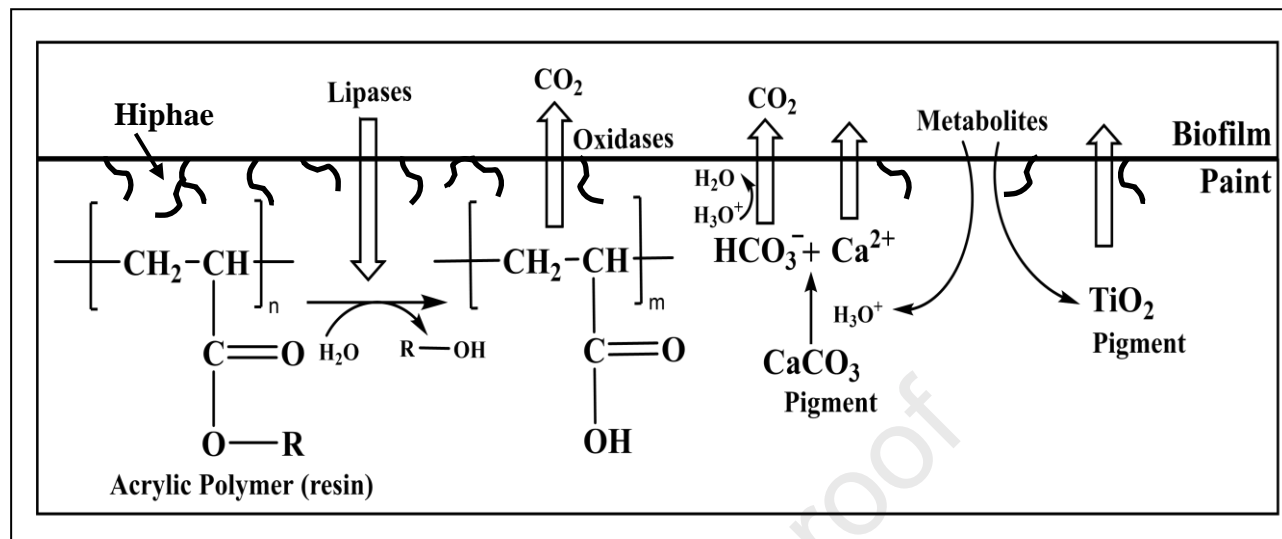


Figure 7

a)



b)

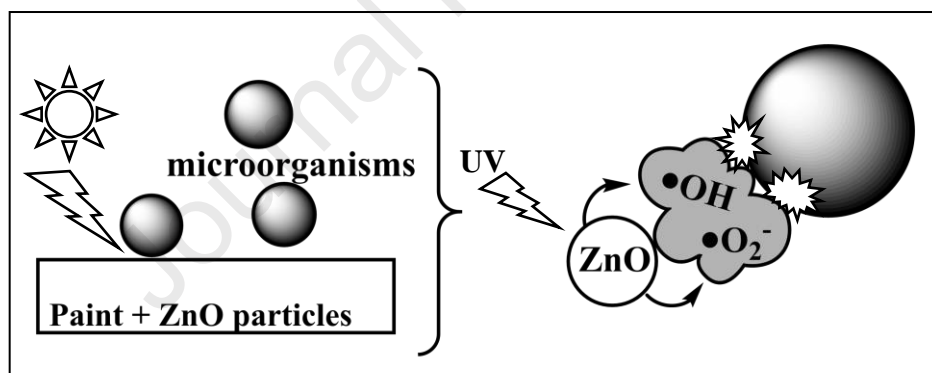
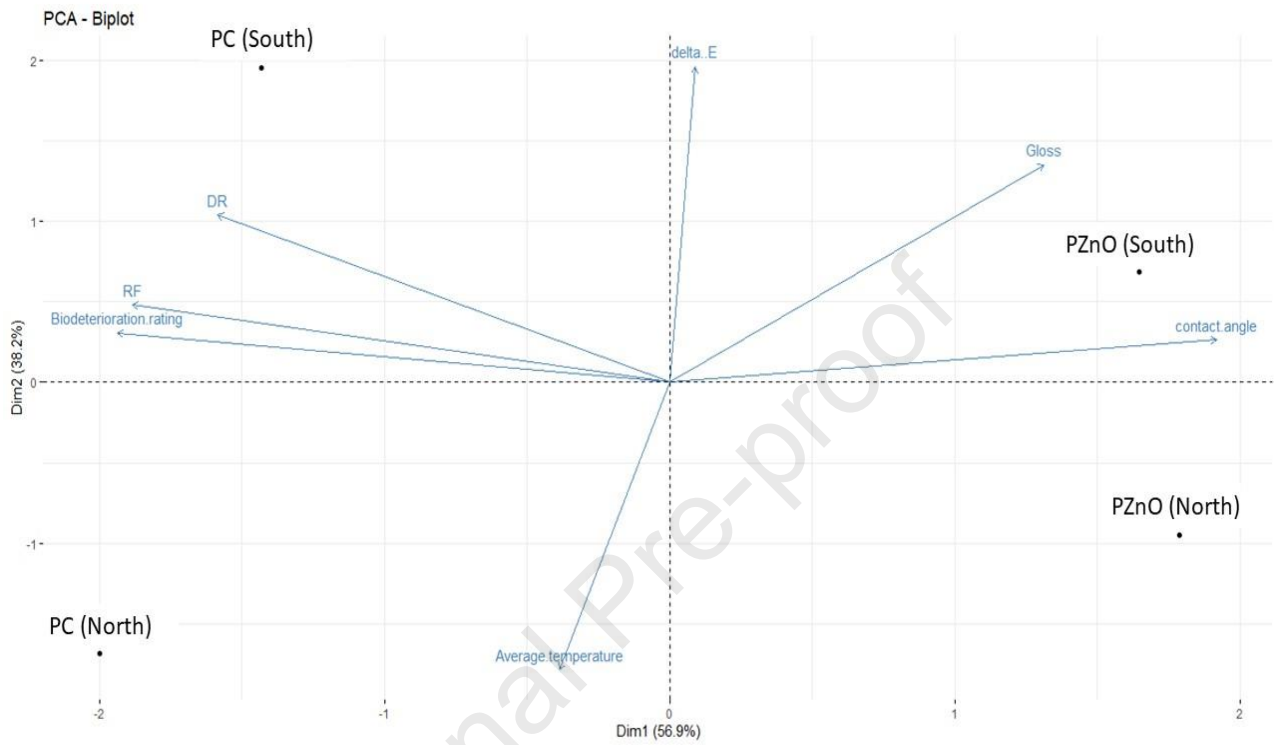


Figure 8



Highlights

An acrylic paint with a photoactive nano-additive was subjected, for the first time, to four year long-term field study.

The additive extended the service life of the coatings due to its antimicrobial activity.

The ZnO particles were the key to biodegradation control.

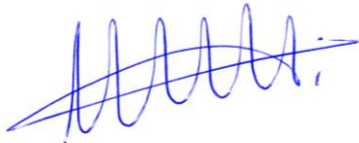
The functionality of the additive in the films was affected by the sample orientation.

The paper has not been published before in any form.

It is not under consideration by another journal at the same time as **Journal of Building Engineering**.

All authors approve of its submission to **Journal of Building Engineering**.

Conflict of Interest: The authors declare that they have no conflict of interest.

A handwritten signature in blue ink, consisting of several loops and a long horizontal stroke extending to the right.

Dra. Natalia Bellotti (CONICET)

CIDEPINT (CICPBA-CONICET-UNLP), La Plata, Argentina

Journal Pre-proof

Author Statementes

Lic. Erasmo Gámez-Espinosa: Methodology, Investigation, Writing-Review & Editing

Dra. Cecilia Deya: Methodology, Supervision, Resources, Writing-Review & Editing

Dr. Facundo Ruiz: Investigation, Writing-Review & Editing

Dra. Natalia Bellotti: Conceptualization, Methodology, Resources, Supervision, Writing Original Draft, Visualization, Project

Journal Pre-proof

Declaration of interests

The authors declare that they have no known competing financial interests or personal relationships that could have appeared to influence the work reported in this paper.

The authors declare the following financial interests/personal relationships which may be considered as potential competing interests:

Journal Pre-proof